Robust superhydrophilic attapulgite-based aligned aerogels for highly efficient and stable solar steam generation in harsh environment

Liang Song[‡,1], Le Geng[‡,1], Yan-pei Tian[1], Peng Mu[*,1], and Jian Li[*,1,2]

[1] Key Laboratory of Eco-functional Polymer Materials of the Ministry of Education, College of Chemistry and Chemical Engineering, Northwest Normal University, 967 Anning East Road, Lanzhou 730070, P. R. China.
[2] Joint Laboratory of Advanced Biomedical Materials (NFU-UGent), College of Chemical Engineering, Nanjing Forestry University (NFU), Nanjing 210037, PR China.

[‡] These authors contributed equally.

* E-mail: pengmu2019@nwnu.edu.cn (P. Mu); Tel: +869317971533.
* E-mail: jianli83@126.com (J. Li); Tel: +869317971533.

Characterization

The microstructure and morphology of the APN and APNP were characterized by a field emission scanning electron microscopy (FE-SEM, Ultra Plus, Zeiss). The chemical composition and function groups were analyzed by FTIR spectra (Bio-Rad FTS-165). The crystal structures of the ATP, APN, and APNP were also examined by an X-ray diffractometer (XRD, Rigaku Corp., Cu Ka, and D/max-2400). The UV-VIS-NIR absorption was conducted at UV-VIS-NIR spectrometer Lambda 750 from 200~2500 nm equipped with an integrated sphere. The contact angle of the APN, APN-PPy, and APNP was measured by contact angle apparatus (SL200KB). The pore structures and Brunauer Emmett Teller (BET) surface areas of resulting the APN aerogel were measured using a micromeritics (ASAP 2020M). All samples were degassed at 120 ^{o}C overnight under vacuum before analysis. The thermal conductivity of APN aerogel was investigated by Netzsch laser flash apparatus CapeL method with model at 40 ^{o}C (LFA457). The longitudinal compressive stress–strain of the APN aerogel was tested using a material testing machine with a 2000 N load cell at a stress rate of 5 mm·min^{-1} (Liangong testing machine, China). The density of the APAC (ρ) was calculated by the ratio of mass (m) and volume (v) using the equation of $\rho = m/v$.

Solar steam generation test

The solar steam generation experiments were conducted at a lab-made, online, real-time measurement system which is consists of a light simulation system and a detection system. The light simulation system including a solar light simulator (Xenon arc lamp, CEL-S500, Ceaulight) with a solar filter (AM 1.5, Ceaulight) and a light intensity was measured by a full spectrum optical power

meter (CEL-NP2000-2, Beijing Education Au-light Co., Ltd.) The detection system including a test chamber is an open cylinder with 80 mm in height 30 mm in diameter, an analytical balance (FA 2004), a computer to record the time-dependent mass change of water due to the stream generation and an infrared camera (Testo 869, Germany). During all tests, the room temperature was maintained at 23 - 25 ℃ and the humidity was ranged from 30 and 35%.

Evaporation test details

(Salt resistance performance) The APNP aerogel was soaked directly in different concentration NaCl solution (3.5%, 5%, 10%, 15%, and 20%), and measured under light simulation system to evaluate the salt resistance performance.

(Acid/pH =1&Alkali/ pH =13 resistance performance) The APNP aerogel was soaked directly in corresponding solution (H_2SO_4/pH =1&NaOH/ pH =13), and measured under light simulation system to evaluate the Acid & Alkali resistance performance.

(Hot water resistance performance) The APNP aerogel was treated with hot water (50 ^oC) of 3h, and soaked in pure water and measured under light simulation system to evaluate the hot water resistance performance.

Calculation of the energy conversion efficiency

$$ŋ=mh_{Lv}/C_{opt}q_i \quad \text{S1}$$

where m is the mass flux of steam (the rate of water evaporation under the dark environment is subtracted), C_{opt} is the optical concentration, q_i is the nominal direct solar irradiation 1 kW m^{-2}, h_{Lv} denotes total enthalpy of liquid-vapor phase change (including sensible heat and phase-change enthalpy), can be calculated as

$$h_{Lv}=\lambda+C\Delta T \quad \text{S2}$$

where λ is latent heat of phase change (The latent heat varies from 2430 kJ/kg at 30 °C to 2265 kJ/kg at 100 °C), C is specific heat capacity of water (4.2 kJ $kg^{-1}\cdot K^{-1}$), and ΔT denotes the temperature increase of the water.

Calculation of the light absorption ability

The light absorptivity of the membrane can be calculated by using the equation:

$$A = 1\text{-}R\text{-}T \quad \text{S3}$$

where *A* is the absorbance, *R* is the reflectance, and *T* is the transmittance.

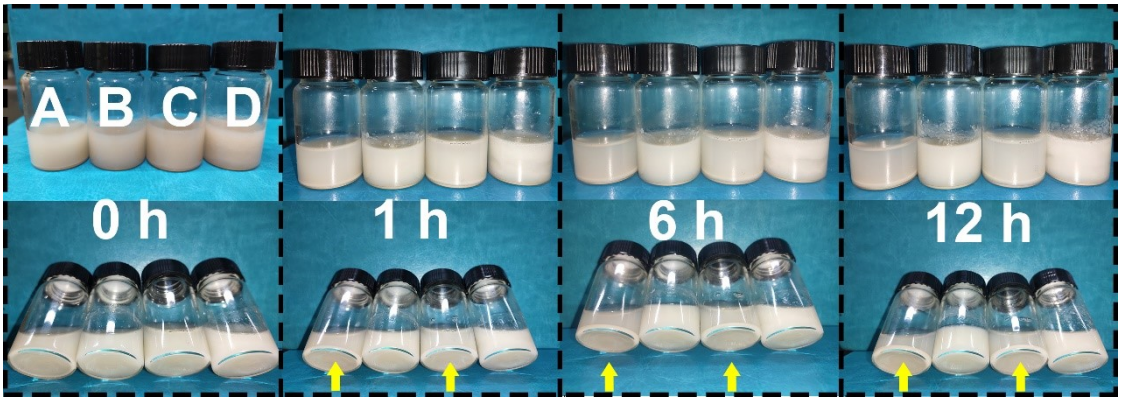

Figure S1 Stability test of (A) ATP+H_2O, (B) ATP+ H_2O+NFC, (C) ATP+H_2O+PVA, (D) ATP+H_2O+NFC+PVA. The feed ratio meets the requirements in the article, and the rest is replaced by water. We can see clearly from the above photos, after 1 hour, the precipitation phenomenon has appeared in solution (A) and (C), and the precipitation gradually increased over time. Oppositely, solution (B) and (D) has no obvious precipitation within 12 hours. This phenomenon indicates that the addition of NFC helps to stabilize the solution, and the addition of PVA will not affect the stability of the solution, which will help the crosslinking of PVA and GA in the next stage to strengthen the network structure.

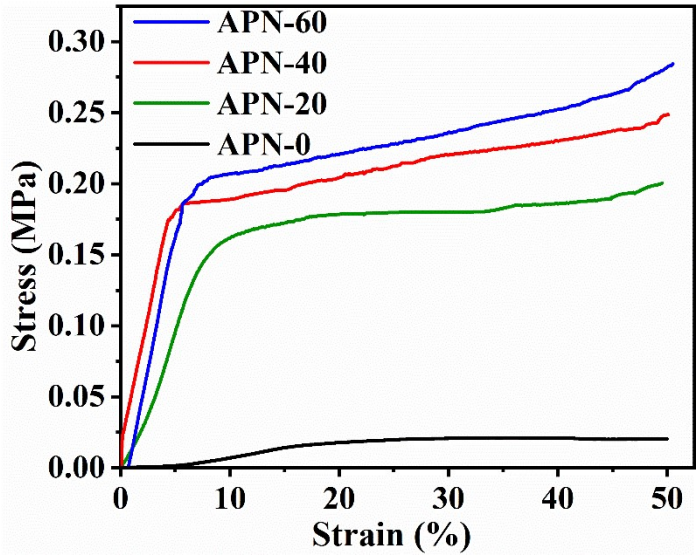

Figure S2 Compressive stress–strain curve of APN-0, APN-20, APN-40, and APN-60 aerogel.

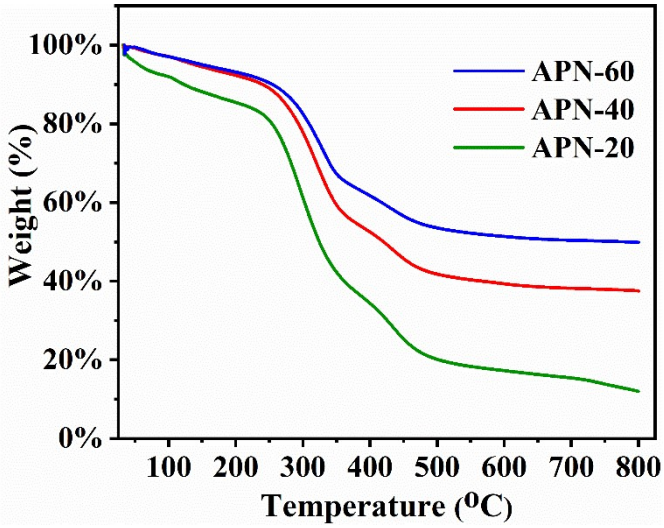

Figure S3 TGA curves of the aerogel of APN-20, APN-40 and APN-60.

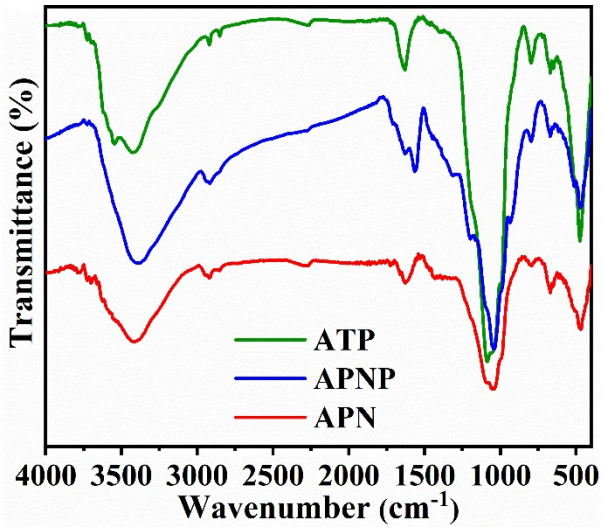

Figure S4 (a) FT-IR spectra of the natural ATP, APN aerogel, and APNP aerogel. After coating with polypyrrole, the APNP with the peaks at 799 cm^{-1} and 932 cm^{-1} attributed to C-H wagging, peak at 1158 cm^{-1} indicative of =C-H in plane deformation vibration, peak at 1194 cm^{-1} attributed to C-H in and out of plane deformations. The absorption at 1313 cm^{-1} and 1562 cm^{-1} were assigned to stretching C-N vibration and -C=C- stretching in the pyrrole ring.[1-3] These different peak signals observed in FTIR indicate that the polypyrrole was successfully coated.

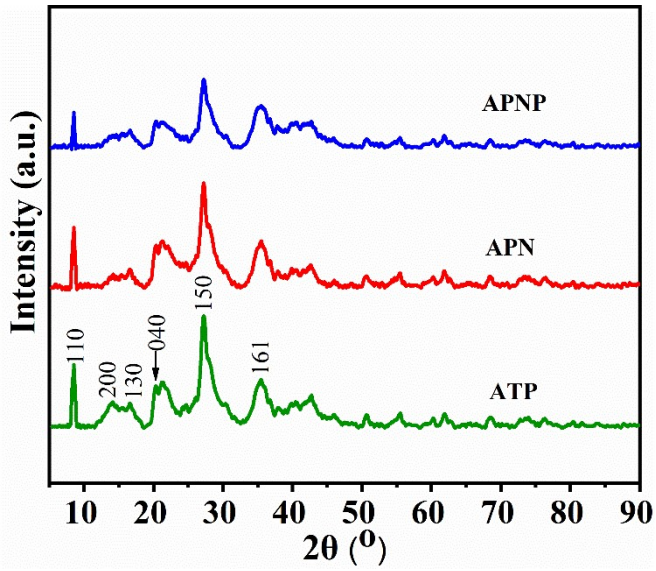

Figure S5 XRD patterns about natural ATP, APN aerogel, and APNP aerogel.

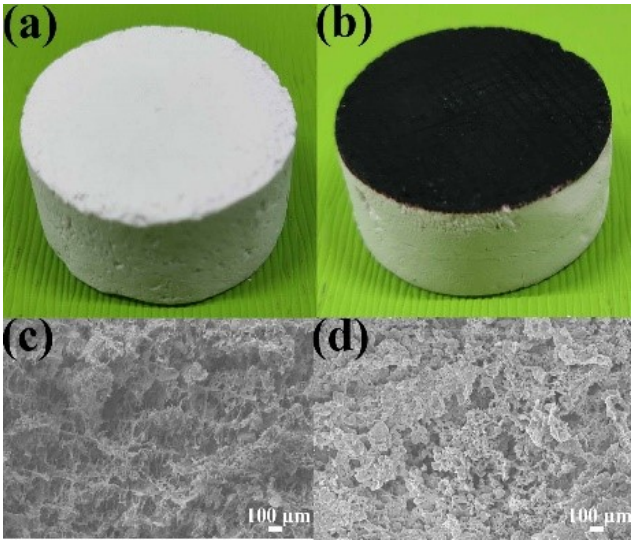

Figure S6 Digital photographs of the (a) APN and (b) APNP aerogel. Scanning electron microscopy images of the (c) APN and (d) APNP aerogel.

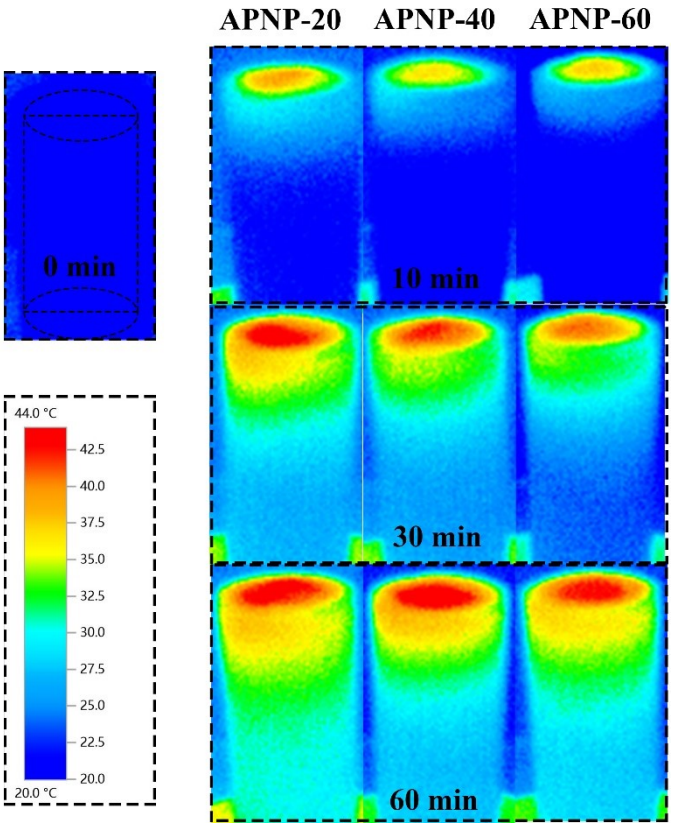

Figure S7 The cross-section temperature distributions of the aerogel of APNP-20, APNP-40, and APNP-60 during solar steam generation under different time.

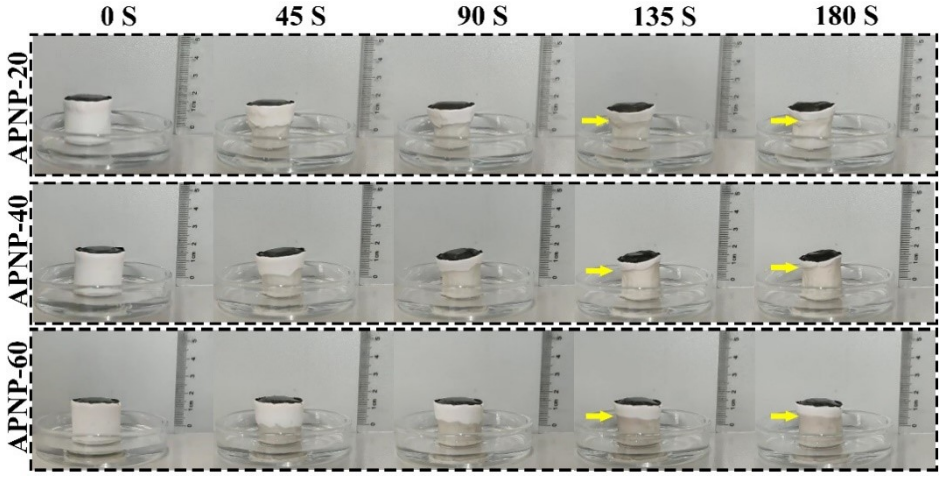

Figure S8 The water permeability of the aerogel of APNP-20, APNP-40, and APNP-60 under different time.

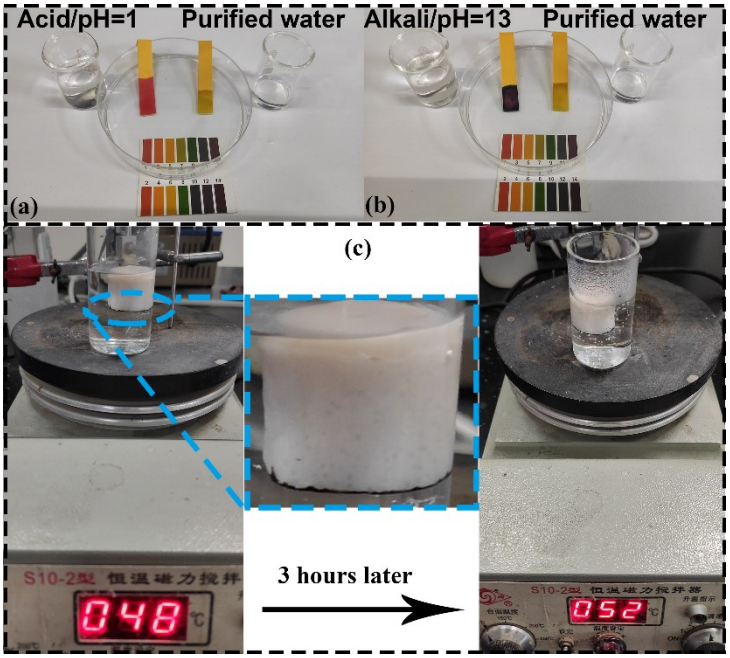

Figure S9 the pH test of purified water after evaporation under (a) acid and (b) alkali solution. (c) the treatment of APNP aerogel under hot water of 3 hours.

Table S1 The density and stress of APN aerogel with different content ATP.

Sample	ATP content (%)	Density (g/cm^3)	Stress (MPa)
APN-20	20	0.041	0.20
APN-40	40	0.049	0.25
APN-60	60	0.060	0.28

Table S2 Thermal conductivities of both dry and wet APNP aerogels at 40 °C

Sample	APNP-20	APNP-40	APNP-60
Dry state	0.157	0.241	0.267
Wet state	0.525	0.475	0.453

References

1. Qi, G.; Wu, Z.; Wang, H., *J. Mater. Chem. C* 2013**,** ***1***, 7102-7111.
2. Shi, K.; Zhitomirsky, I., *J. Mater. Chem. A* 2013**,** ***1*** (38), 11614-11623.
3. Navale, S. T.; Mane, A. T.; Ghanwat, A. A.; Mulik, A. R.; Patil, V. B., *Measurement* 2014**,** ***50***, 363-369.